The Report committee for Joseph Frederic Tansey

Certifies that this is the approved version of the following report:

Pore Network Modeling of Carbonate Acidization

Approved by Supervising Committee

_____

Matthew Balhoff, Supervisor

_____

Kamy Sepehrnoori

Pore Network Modeling of Carbonate Acidization

By

Joseph Frederic Tansey, B.S.P.E.

Report

Presented to the Faculty of the Graduate School

of the University of Texas at Austin

in Partial Fulfillment

of the Requirements

for the Degree of

Master of Science in Engineering

The University of Texas at Austin

May 2015

Acknowledgments

I would like to thank Dr. Matthew Balhoff, Dr. Murtaza Ziauddin, Dr. Maša Prodanović, Dr. Karsten Thompson, Yashar Mehmanni, Tie Sun, Timothy Thibodaux, and Schlumberger for their guidance, enthusiasm, and support of my research.

Pore Network Modeling of Carbonate Acidization

by

Joseph Frederic Tansey, MSE

The University of Texas at Austin, 2015

Supervisor: Matthew Balhoff

Over half of the world's hydrocarbon reserves are found in carbonates. Acid injection is a cost effective way to enhance productivity in carbonates by reducing the near-wellbore skin. Ideally, injected acid creates highly permeable channels around the wellbore, known as wormholes. The successful formation of these wormholes depends on acid type, injection rate, and reservoir properties. Improper treatment design results in sub-optimal acid placement with negligible permeability increase. Previous attempts to accurately capture the wormholing process using a pore-scale network model have encountered many difficulties. We present a modern pore network model of carbonate acidization using networks extracted from CT scans of carbonate cores. A mass transfer coefficient and pore merging criterion are developed using finite element simulations in COMSOL that both greatly improve network physics. While there are many weaknesses to the pore network modeling approach, the optimal Damkohler number for our networks closely matches experimental data.

Contents

Table of Figures

Introduction

Optimization of acid placement during matrix acidization is important for maximizing increases in near-wellbore permeability. Many models describe this process, and either fall short or else require many experimental inputs. A pore network model of carbonate acidization only requires a descriptor of the pore space, which can be obtained from CT scans of extracted cores. Unfortunately, past pore network models of matrix acidization have failed to quantitatively capture the phenomenon. The hypothesis of this research is that pore network models covering a large enough domain and with more descriptive physics will succeed in matching experimental results. The specific research objectives are as follows:

1. Use CT scans of carbonate cores to create many physically representative pore networks
2. Simulate matrix dissolution on a single network
3. Use mortar coupling to simulate matrix dissolution on a much larger domain size comprised of many networks
4. Obtain optimal injection strategies for a variety of fluid/rock systems at both core and field scale.
5. Extend results to non-Newtonian fluids, particularly viscoelastic fluids

Literature Review

Field Practice

Matrix acidization has been employed extensively in a variety of applications. Hydrofluoric acid is used to remove near wellbore damage in sandstone reservoirs (Smith and Hendrickson, 1965). Acid fracturing is used in low permeability carbonate reservoirs to create long, acid-etched fractures (Navarrete et al., 1998). Most frequently, however, is the use of strong acids such as HCl to enhance the near-wellbore in moderate-high permeability carbonates. In the ideal case, highly conductive wormholes are formed, reducing near wellbore skin, and therefore increasing the permeability of the rock. In practice, improper stimulation design can result in lackluster productivity due to inefficient placement of the acid (Thomas et al., 1998). Field stimulation strategy is also constrained by factors such as the maximal injection rate (Huang et al., 2000). Choice of fluid type, injection rate, and injection concentration are key design parameters to maximize the stimulation effect (Wang et al., 1993).

Acidizing Characterization

Wormholes are believed to form because of the natural heterogeneity of carbonates, whereby acid flows preferentially through high-permeability pathways, enlarging them, and in turn diverting more acid to themselves (Golfier et al., 2001). Dominant channels form which provide negligible resistance to flow around the wellbore. Productivity increases observed in field conditions vary widely. Al-Dahlan et al. (2000) recorded a tripling of the injectivity index in a carbonate water disposal well. Mohamed et al. (1999) studied over 80 water injectors in carbonate reservoirs treated with hydrochloric acid below the fracture gradient. They found injectivity increased by approximately a factor of two.

An intermediate injection rate is believed to create wormhole patterns in the matrix. Injecting too slowly results in “compact dissolution” around the wellbore face and a negligible permeability increase. Injecting too quickly disperses the acid out into the formation, resulting in poorly connected “uniform dissolution” (Figure 1).

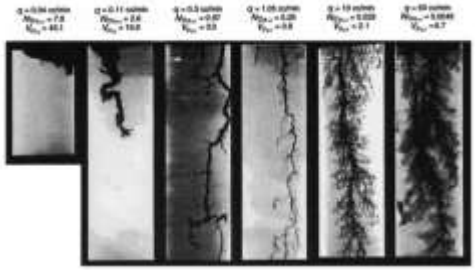

Figure 1: Cross Sectional View of Acidized Cores. Compact dissolution (left), Wormholing (middle), Uniform Dissolution (right). (Fredd and Fogler 1998a)

Core flood experiments have consistently shown optimal injection rates for a variety of fluid-rock systems. Fredd and Fogler (1998b) measured breakthrough trends for limestone cores using conventional acids (HCl, HAc) as well as strong chelating agents (CDTA, DTPA, EDTA), and showed their behavior collapsed into similar curves if plotted versus the Damkohler number (Figure 2).

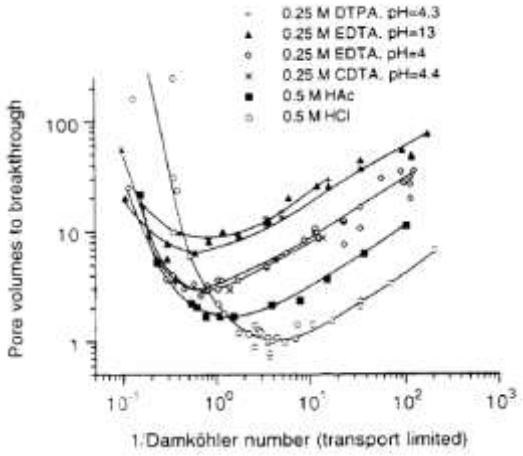

Figure 2: Breakthrough Using Various Acidizing Fluids. (Fredd and Fogler, 1998b)

The Damkohler number is defined as the ratio of the net rate of dissolution by acid to the rate of convective transport of acid for both mass transfer and reaction rate limited regimes respectively (Equations 1 and 2), where D_e is the effective diffusion coefficient $(length^2 time^{-1})$, is the pore length $(length)$, d is the pore diameter $(length)$, k_r is the surface reaction rate constant $(units\ depend\ on\ order\ of\ reaction)$, and a is a constant that depends on the carbonate core whose units vary in both equations such that the Damkohler number is dimensionless.

$$Da_{mt} = \frac{aD_e^{\frac{2}{3}}l}{Q}, \quad (1)$$

$$Da_{rxn} = \frac{ak_r dl}{Q}. \quad (2)$$

Thus, the Damkohler number depends on both the injection rate and concentration of acid. An optimal Damkohler number of 0.29 was observed for the studied fluid/rock systems. Unfortunately, the Damkohler number as described by Fredd and Fogler (1998b) cannot be obtained *a priori*. At the macroscopic scale, it must be calculated after the experiment has concluded. The final dimensions for wormhole diameter and length are substituted for pore diameter and length. Both of these parameters are extremely difficult to quantify in a consistent manner.

Numerous authors have attempted to obtain a general criterion or expression for the optimal injection rate. A transition pore-size approach was formulated by Wang et al. (1993). Semi-empirical relations were presented by Gong and El-Rabaa (1999) and Talbot and Gdanski (2008), which showed good agreement with experiments, but require many laboratory measurements.

Models of the Acidizing Process

Many models have been proposed that qualitatively and quantitatively capture the acidizing process. Early capillary tube models captured the propagation of wormholes under rigid assumptions. Schechter and Gidley (1969) studied the evolution of pore size distribution by considering an array of short cylinders distributed randomly throughout a solid. Glover et al. (1973) experimentally verified Schechter and Gidley's predicted change in pore size distribution by using sintered glass disks. Hung et al. (1989) modeled the wormhole as a growing cylindrical tube inside a solid core, using Darcy's law coupling the wormhole/core interface. The core grows in width and length as acid is injected. Results show increasing wormhole length with increasing injection rate. Simulations on growth of multiple wormholes suggest that a dominant wormhole is more likely with a high diffusion rate or a low fluid-loss rate. No experimental comparisons were given. Walsh et al. (1982) modeled the effect of acidization and precipitation on permeability for various minerals, using a semi-empirical relationship between permeability and porosity. Their results correlate well with experimental data, although no acidizing regimes are produced. Walsh et al. (1984) extended this work in porous

media using a 1D reactive model, successfully predicting the distribution roll-front uranium deposits. Huang et al. (1997) extended this capillary model to field conditions using Darcy's law in radial flow, concluding that fluid loss from wormholes in field treatments exceeds that found in linear corefloods, thus overpredicting wormhole formation in field conditions.

Several Darcy-Scale models have been used to describe the dissolution process. Bekri et al. (1995) used a Darcy scale model to study evolution of deterministic channels and close packs of cubic sphere arrays, and observed wormholing along preferential pathways. Where most work neglects the precipitation process in acidizing, Quinn et al (2000) showed that the precipitation process substantially impacted acidizing effectiveness. A finite-difference Darcy scale model was used, and permeability changes correlated to changes in porosity due to specific mineral reactions via a modified Carman-Kozeny relation. Optimal injection strategies are presented, although no direct experimental breakthrough comparisons are made.

Golfier et al. (2002) present a 3-D Darcy scale model using 201x101 nodes. Individual blocks are assumed to have a homogeneous permeability. A fixed relationship between porosity and permeability is chosen. The model is able to capture the characteristic dissolution regimes, and with the selection of appropriate length scales, reproduces the optimal Damkohler number of around 0.29 from Fredd and Fogler (1998b). The model is very sensitive to the choice in mass transfer coefficient, whose selection depends on an arbitrary shape-factor coefficient and the local Péclet number. Their optimal Damkohler number is identified on the basis of maximizing wormhole length, rather than reaching a permeability threshold.

Panga et al. (2005) employed a 2-D two-scale continuum model to simulate the dissolution process. Changes in local permeability are correlated to porosity using a semiempirical formula, which requires an average pore radius and interfacial area. The model shows good agreement with breakthrough curves for salt packs after calibration with experimental data. Maheshwari and Balakotaiah (2013) extended this two-scale continuum model to 3-D. Mesh size is set at 180×72×72 in a rectangular lattice. Results show excellent agreement when compared to the limestone-HCl system from Fredd and Fogler (1998b). Variations in simulation heterogeneity reveal that wormhole branching increases with increasing heterogeneity, and that there exists an "optimum" heterogeneity that minimizes breakthrough time.

The primary shortcoming of continuum models is the difficulty in capturing pore-scale heterogeneities. Heterogeneity is introduced artificially as deviation from some mean

porosity, rather than reflecting real variations in rock quality. Additionally, even the best continuum models must rely on porosity-permeability correlations obtained experimentally or using simple analytical relations, further homogenizing the simulation under the assumption that all porosity changes translate into a predetermined amount of permeability. Thus, existing continuum models lack the ability to directly simulate complex pore structures. Up-scaling of laboratory reaction rates to the continuum scale is also problematic in the context of matrix dissolution. Lichtner and Tartakovsky (2003) found that volume-averaging methods to upscale reaction rate constants for quartz dissolution resulted in effective reaction rate constants that varied as a function of time, which they attributed to heterogeneous distribution of grain sizes.

The Lattice Boltzman Method (LBM) has also been applied to the acidizing process. Kang et al. (2002) used the LBM on 3D cross sections measuring approximately 0.5mm in length. The Navier-Stokes equation is solved over each voxel, and coupled with a simple transport and reaction model. Dissolution by 0.5M HCl and HF is performed. No comparisons with experiments are made. However, the number of pore volumes to breakthrough is significantly closer than most other *a priori* models. Optimal injection strategies are obtained, although no clear dissolution regimes are presented. Szymczak et al. (2009) also employed the LBM to study the evolution of wormhole channels in fracture surfaces textured with randomly placed objects. Experiments on homogeneous fracture planes (essentially 2D) were used to validate the LBM. The characteristic dissolution regimes are reproduced, and optimal injection rates obtained. Mass transfer limited regimes were found to produce the most channeling, although no direct comparison to acidizing experiments is given. The major drawbacks of LBM are the extremely small (likely unrepresentative) domain size and long computation times. It is not practical to use LBM to simulate dissolution on significant samples of cores.

Pore Network Models of Carbonate Acidization

We use pore-network modeling to capture essential physics where continuum models cannot. The first network model of a porous media was used by Fatt (1956) to study multiphase characteristics of pore space. Pore network models have since been used to study a variety of complex petrophysical phenomena. Bryant et al. (1993) generated networks from disordered sphere packs that accurately predicted single phase permeability. Li et al. (2006) used a pore network to model reactive transport of CO_2. They assumed perfect pore-level mixing and a simple reaction rate law. They observed significant discrepancy between reaction rates predicted by continuum- scale models compared to their pore network model. For example, at steady state, the continuum model underestimated kaolinite precipitation by almost two orders of magnitude. The authors

attribute this discrepancy to the highly heterogeneous local reaction rates that occur because of non-uniform dispersion of reactant in the network.

Network models have been applied to study matrix acidization. Hoefner and Fogler (1989) used a 2-D network consisting of a regular triangular lattice of 40 × 40 nodes. Hagen-Poiseuille flow is assumed between nodes, with reaction enlarging the connecting throats. The three primary dissolution regimes (Face, Wormhole, and Uniform) are observed, but no quantitative experimental comparisons are made.

Fredd and Fogler (1998b) present a 3-D physically representative network model using a packed bed spheres with variable size. Delauny tessellation of the spheres is used to identify pore centers and throats. Conductivity between pores is calculated numerically using the solution for hyperbolic venturi. Pore scale mass-transfer is modeled using a Hagen-Poiseuille relationship (assuming an effective radius such that the conductivities match that of the actual pore throats). Reaction is carried out according to a local Damkohler number based on throat dimensions. The spherical grains are allowed to shrink under dissolution, increasing pore volume. Merging of pores is purportedly facilitated by the fact that grains can completely dissolve, although the network maintains its structure and fixed coordination number. The dissolved throat maintains its radius and continues to provide resistance to flow even when the surrounding matrix is completely dissolved.

Simulations were performed on networks of approximately 3300 pores and 0.1 cm length. They reproduce the expected dissolution regimes and provide breakthrough curves for different fluids which collapse on top of each other when normalized by their macroscopic Damkohler number. Unfortunately, the simulations over predict the optimal injection rate by more than a factor of 10. The authors claim that small domain size and unrealistically permeable networks are major sources of error. A larger domain size is likely to improve results, since even the thinnest wormhole diameters are substantially larger than pore networks. Additionally, more realistic pore networks (rather than sphere packs) that capture local heterogeneity are likely to accentuate wormhole formation via the enlargement of already conductive flow paths.

Up-Scaling Techniques

Larger domain sizes can be reached by using domain decomposition techniques such that the problem can be partitioned and sent to multiple processors and solved quickly. Many networks can be “glued” together using mortar coupling. Mehmani et al. (2012) used mortar coupling to simulate reactive transport of CO2 in 64 separate pore networks coupled as one large domain (Figure 8). Precipitation of reactants reduced throat sizes

and therefore permeability. A variety of precipitation regimes were observed for different injection conditions. Results were demonstrated to be very accurate when compared to non-mortar solutions. Simulations were completed in a single quad core computer, implying that much greater domain sizes can be easily reached using computing clusters.

Larger domain sizes also enable field-scale simulations. Cohen et al. (2008) found that simulations in radial geometries showed higher optimal injection rates than in linear core flood cases, suggesting that simple linear simulations are inapplicable to field conditions. Sun et al. (2012) modeled a ~1 m^2 pore-scale region around a single-phase producing well coupled to larger scale Darcy blocks using over 7500 pore scale models coupled using finite-element mortars. Sun showed that local pore scale heterogeneities significantly influenced the pressure field and flow path around the wellbore, implying that continuum models would poorly predict acid placement. Additionally, Bartko et al. (2007) found that perforations produce straighter and stronger wormholes than the unperforated (homogenous) case, implying that field-scale simulations of matrix acidization might benefit from including perforations near the wellbore.

Non-Newtonian Fluids

Non-Newtonian fluids are also of interest for their ability to improve acid placement in formations. Lungwitz et al. (2007) studied a viscoelastic acid system in core floods that increases in viscosity as acid is spent. While self-diverting fluids are typically thought to be most useful in acid-fracturing applications, Majdi et al. (2003) found that visco-elastic self-diverting acid was highly effective for matrix acidizing in a field study involving multi-layered carbonate structures (3md to 400md). The authors claim that diversion of acid away from highly permeable zones results in better acid coverage, and report productivity increases of 2-4 in all 17 wells treated. Similarly, Nasr-El-Din et al. (2006) reported a 95% success rate of 20 wt% hydrochloric acid system with viscoelastic surfactant in conventional carbonate reservoirs. Afsharpoor et al. (Pending) obtained a pressure equation for viscoelastic fluids for use with pore network models. The pressure term is broken up into viscous and elastic components to form a nonlinear system of equations. The results from the network model are validated with experimental results on bead packs, thus implying suitability for carbonate networks.

Project Overview

The objective of this work is to accurately model acidizing of carbonates at the pore scale to obtain quantitative agreement with experiments and general validity. Specifically, we have created pore network models from real carbonate core scans, validated networks against tracer test experiments, and simulated matrix dissolution to obtain characteristic dissolution patterns and breakthrough curves.

Pore-Network Extraction

CT scans of small cores have been provided by collaborators at Texas A&M, DOE, and Schlumberger. Several small cores have also been provided by Schlumberger to be scanned at UT's High Resolution X-ray CT Facility. Schlumberger has also scanned carbonates using their own in-house CT scanner and made them available for use in this research. Experimental data is available for most of the cores/scans that Schlumberger has provided.

The raw image slices are segmented into grain and pore space using Indicator Kriging (IK) in 3dma_Linux. This technique requires an *a priori* cutoff value for grain and pore space. A histogram of intensity values was obtained (Figure 3), and thresholds were selected such that intermediate "grey area" could be determined. Figure 4 shows the 2D images of the rock sample.

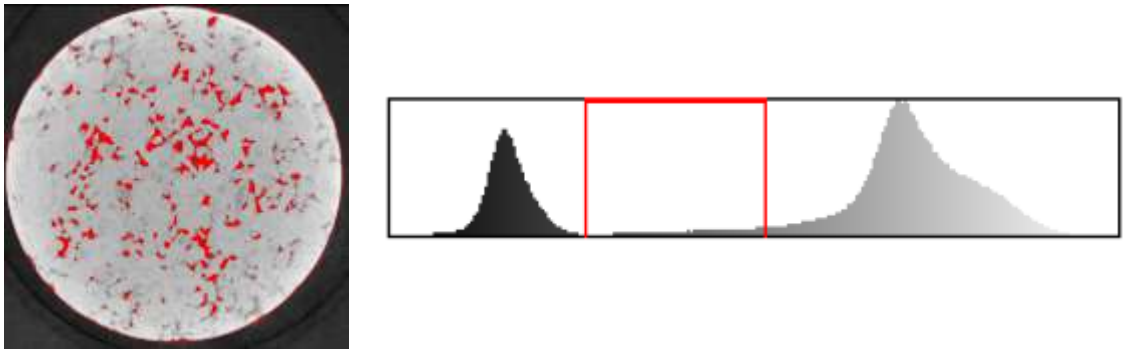

(a) (b)

Figure 3: Segmentation of Greyscale CT Scan. Figure 3a left: Greyscale image of CT scan with indeterminate voxels highlighted in red. Figure 3b shows a histogram of intensity values from the scan. The leftmost peak corresponds to void space, and the rightmost peak corresponds to grain space. The intermediate values (highlighted in red) will be assigned to grain/void during Indicator Kriging based on their spatial relation to other voxels.

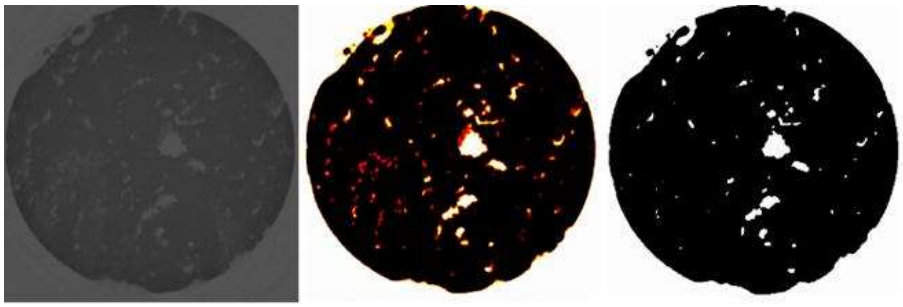

(a) (b) (c)

Figure 4: Segmentation Process of a Thin Section (a) Original image, (b) selection of intermediate thresholds, and (c) final binary image.

Binary voxel space was then constructed from the slices (Figure 5), and used as an input for a network extraction algorithm. We have access to two such algorithms; 3dma_Linux from Dr. Prodanović at UT, and another from LSU. From either code, the resulting network model consists of pores and connecting throats and is a one-to-one mapping of the original porous medium (Figure 6). Pore Geometry, location, and throat conductivities are examples of information quantified for use in transport simulations.

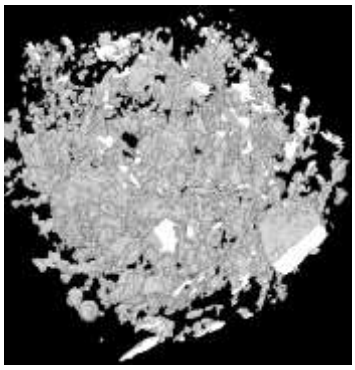

Figure 5: Binary Voxel Space of a Carbonate core

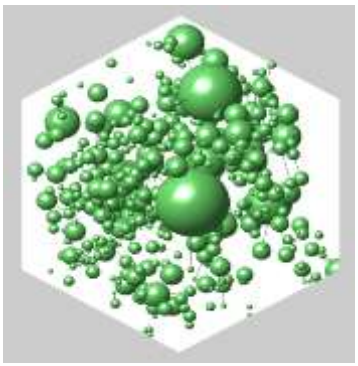

Figure 6: Network extracted from Voxel Space

We are currently employing LSU's network extraction algorithm. A medial axis is traced through the pore space of the medium. The medial axis path is a skeleton of connected lines through the pore space whose segments are equidistant from at least two different points on the object border. A pore is defined as the intersection of three or more paths, and the radius is checked based on the maximum sized voxel-sphere that can be grown before hitting the grain boundaries. A similar dilation method is used to calculate the inscribed radii of pore throats. Throat conductivity is calculated using methods from Patzek and Silin (2001), whereby irregular throat shapes are mapped onto triangular, square, and circular geometries, depending on their shape factors.

Pore Network Model

In order to solve the transport and dissolution process, we employ an implicit pressure, explicit concentration (IMPEC) approach in which we first solve for pore pressures and flow rates and then solve for species concentration in each pore at a given time step. The specific steps in the time-dependent scheme are summarized as follows:

1. Solve for the pressure and flow field in the network
2. Update pore concentrations using an operator splitting approach (advection and reaction)
3. Compute pore volume change and throat conductivity increase
4. Calculate increased porosity and permeability in the network model
5. Advance to next time step and repeat

Pressure Field

The pressure field is solved by enforcing mass balance over each pore, assuming creeping, single phase, Newtonian flow. Equation 3 is written for each pore, where Q_i is the net flow in/out of pore *i*, q_{ij} is the flow through the throat connecting pore *i* and *j*, $g_{ij}$is the conductivity between pores *i* and *j*, P_i is the pressure in pore *i*, and μ is the viscosity.

$$Q_i = \sum_j q_{ij} = \sum_j \frac{g_{ij}}{\mu}\left(P_i - P_j\right) = 0\,. \tag{3}$$

This system of equations is solved to obtain pressure in each pore. In this way, flow rate through each throat can be calculated. Directional flow rate can be measured by summing flux over each face. Permeability obtained from carbonate networks is typically on the order of 10 md. This is in close agreement with experimental data, although there are currently no networks generated directly from experiment cores.

Species Transport

The pressure field is used to advance species through the network explicitly via the reaction-diffusion-advection equation (Eqn. 4), where V_{p_i} is the volume of pore *i*, c_i is the concentration in pore *i*, $D_m$is the molecular diffusivity, a_{ij} is the cross sectional area of the connecting throat, l_{ij} is the length of the connecting throat, and $R(c_i)$ is the reaction term.

$$V_{p_i}\frac{dc_i}{dt}=\sum_i c_i q_{ij}+\sum_i D_m a_{ij}\frac{\Delta c_i}{l_{ij}}+R(c_i)\,. \tag{4}$$

Only species transport by advection is considered. Diffusion was neglected for computational simplicity, as the pore level Péclet number in the majority of injection rates was computed to be much too high for diffusion to affect species transport. Additionally, in field practice, many acidizing fluids are chosen specifically to minimize the diffusion rate and ensure acid transport to the tips of wormholes.

Flux into and out of each pore carries fluid with concentration equal to the upstream concentration (Eqns. 5 and 6). Timestep is constrained to be no larger than the minimum time required to evacuate a single pore for the given pressure profile in accordance with the Courant-Friedrichs-Lewy (CFL) condition.

$$\Delta C_{convection_i}=\frac{(C_{inlet}q_{ij})\Delta t}{V_{p_i}}\,, \tag{5}$$

$$C_{new_i}=C_{old_i}+\Delta C_{convection_i}\,. \tag{6}$$

Species Reaction

Reaction of hydrochloric acid is simulated in each pore based on a chemical reaction with calcite and hydrochloric acid (Eqn. 7). The change in concentration is proportional to surface area; a rate expression (Eqn. 8) provided by Lund et al. (1974) based on a spinning disk is implemented.

$$CaCO_{3(s)}+2H^+ \rightleftarrows Ca^{2+}+CO_{2(aq)}+H_2O\,, \tag{7}$$

$$r_H=-8.8\cdot 10^{-6}\left(C_{HCl}\right)^{0.63}\,. \tag{8}$$

The new concentration in the pore is then updated as

$$C_i^{n+1}=C_i^n+\Delta C_{reaction_i}\,. \tag{9}$$

Matrix Dissolution

The pore size and throat conductivity are increased according to the stoichiometric ratio of the reactants assuming a grain density of 2.71 g/cc. A total volume of dissolved grain is computed for each individual pore. This dissolved volume is translated into dissolved surface area assuming a spherical pore (using the pore's effective radius). This area is then distributed to each throat's "effective cross sectional area" in proportion to its existing conductivity. This allocation strategy is based off the assumption that the pore body dissolves primarily around the throats, because throats have the largest surface-area-to-volume ratio. Improvements on this approach are discussed in the "Future Work" section.

The throat shape factor between pores is assumed constant as the cross-sectional area of throats increases. Throat conductivities are then updated using the new cross sectional areas. Since throats connect two pores, and can thus grow from both sides, conductivities are checked to ensure they match from both directions. If there is a conflict, the larger conductivity is chosen in order to maintain strictly-increasing permeability.

Finally, a pore-merging algorithm searches for pores that now overlap significantly. Whether two pores "merge" is determined by an arbitrary threshold that compares the amount the radii overlap (currently .35 of the largest radius). If this threshold is met, a new pore is created. Pore volume is the sum of the two previous volumes. Location and concentration are assumed proportionate to original pore volumes. The new pore is connected to all the same "neighbors" of the original two pores at the same conductivities.

Network Model Results

We can validate our extracted network using tracer tests provided by Schlumberger. While no carbonate networks from these specific cores exist at the time, simulation on carbonate networks of comparable permeability and porosity showed good agreement with tracer experiments (Figure 7).

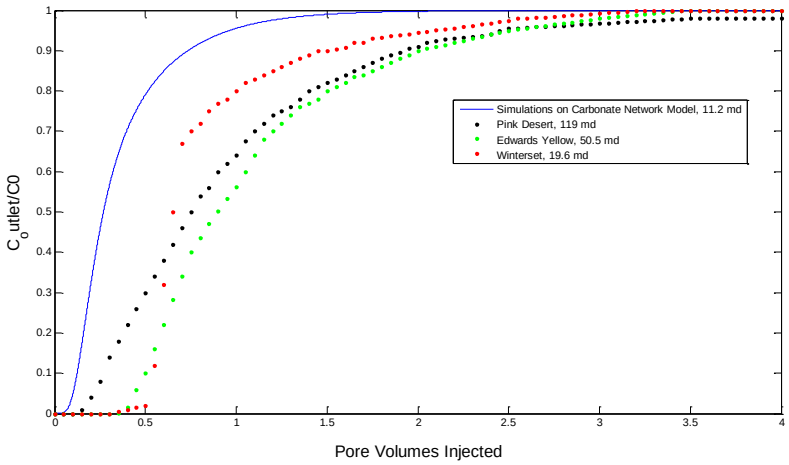

Figure 7: Comparison of breakthrough profiles for experiments and simulations. Simulations on low permeability network best matches low permeability carbonates, albeit from non-matching cores. Networks extracted from experimental cores will be compared in this fashion.

Currently, no breakthrough tests are available for which we have extracted networks. However, simulations run using arbitrary inputs demonstrate expected trends in permeability (Figure 8). A dominant flow path emerges at intermediate injection rates through which acid is diverted (Figure 9).

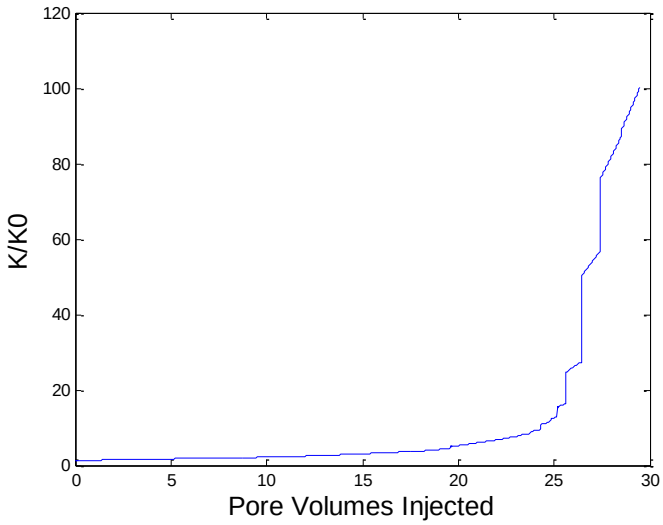

Figure 8: Permeability increase with injected acid for 1000 grain sphere pack

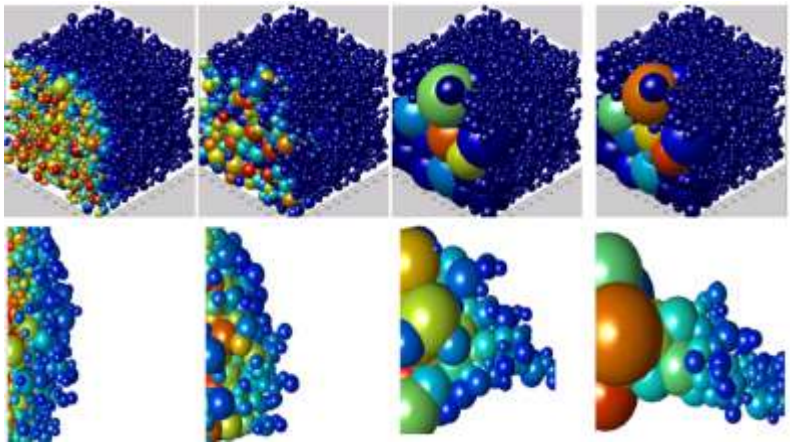

Figure 9: Dissolution of 1000 grain sphere pack network resulting in high-flow conduit under constant injection rate and concentration. Colour "heat" shows acid concentration in a pore. The bottom row of images only show pores with significant acid from an overhead view. Acid is initially distributed uniformly, but diverts into a preferential flow path as the matrix is dissolved.

An optimal injection rate is observed for each network at a specific acid concentration. However the number of pore volumes to breakthrough is much higher than that seen in experiments. Different sized networks are found to have different optimal rates of acid injection, as well as different minimum pore volumes to break through (Figure 10).

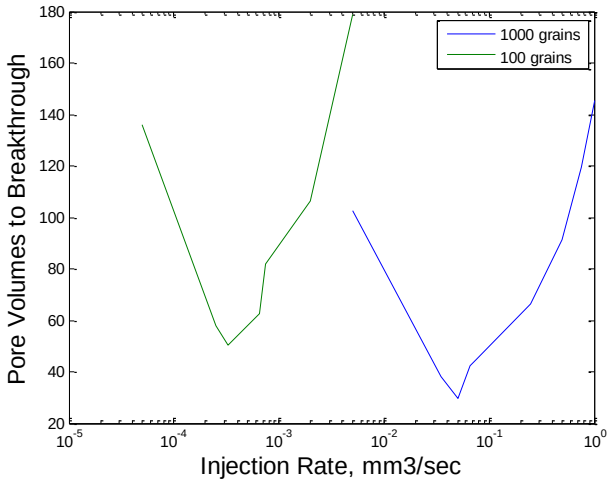

Figure 10: Breakthrough curves for two different sized domains indicates that simulations are likely below the representative elementary volume (REV).

It appears as though small domain sizes require a higher number of pore volumes to break through. Fredd and Fogler (1998) commented that this could be an artifact of the fact that smaller domains are disproportionately dominated by wormholes, since there is so little of the domain unaffected by the acidizing process. Increasing domain size

through mortar coupling is therefore likely to significantly improve agreement with experimental data, which typically shows breakthrough on the order of 0.5-10 pore volumes for HCl.

Model Applications:

Mortar Coupling

It is difficult (or impossible) to create pore-networks the size of a core, and wormholes may extend to length scales much larger than a conventional pore network. Moreover, estimates in the literature show significant boundary effects on core samples smaller than 1"×6", with no dependence on domain size above this critical threshold (Cohen et al., 2008). Simulations on different sized networks of sphere packs here reveal that increasing domain size decreases number of pore volumes to breakthrough. Therefore, we expect that a much larger domain will yield better agreement with experiments.

Coupling hundreds of pore-networks together using mortar coupling techniques allows simulation of behavior at larger scales. Tthe problem can be solved efficiently in a parallel computing environment (Mehmani et al, 2012). Using mortars to couple many networks together to reach the size of a core is would allow a 1:1 domain size comparison with experiments.

It is likely that this will take hundreds or thousands of networks coupled together. Computing power of a single processor may prove insufficient or lead to impractical simulation times if the entire domain is simulated fully. However, only the portion of the domain whose acid concentration is above a certain threshold need be simulated. Under wormholing, this could result in less than 10% of the network requiring full simulation of reaction and dissolution.

Conventional reservoir software, such as Eclipse or Intersect, could be coupled with mortars. Pore networks would replace Darcy-scale blocks around the wellbore and be coupled both to each other and outer Darcy blocks using mortars. Sun et al. (2012) was able to solve single phase pressure for $1m^2$ around the wellbore. The acidizing process could be simulated in a similar manner.

Improve Reactive Model

Current work has focused on HCl using a mass-transfer rate limited model with perfect and instantaneous mixing in individual pores. It is unlikely that this approach will work in the general case for several reasons:

1) Many acid systems are not simply mass-transfer limited. For example, Bazin et al. (1995) found that optimal injection rates for HCl in limestone occurred at the transition between mass transfer and convection rate limited systems.

2) Neglecting intra-pore diffusion creates lots of error when pores become large. Large pores are frequently produced in simulations, particularly during face dissolution (Figure 11). The assumption of perfect mixing effectively creates instantaneous transport of acid very large distances along the network.

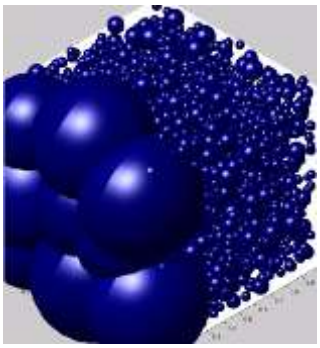

Figure 11: Very large pores formed at low injection rates (face dissolution)

3) Since the pore space is significantly simplified by our network extraction algorithms and subsequent assumptions, there is no way to synthesize real pore geometry with a generalized reaction rate. A generalized reaction rate is not useful if the domain is only roughly characterized.

4) Mass transfer resistance is likely to be significant at the pore scale. Presence of other ions (such as the reaction product Ca^{2+}) could have a large influence on transport of H^{+} to the interface. Experiments, such as the spinning disc experiments our current reactive model is based on, were specifically designed to minimize mass transfer resistance.

For these reasons, a fully empirical relation could be used to capture reaction in the pores. Results from breakthrough experiments (ideally a full permeability vs. time comparison) would allow for the reaction model to be calibrated. The reaction model should be simple enough such that it retains some physical significance. For example, the empirical rate expressions given in much of the literature take the form of equation 10, where r is the reaction rate (mol cm-2 s-1), C is the species concentration (gmol/l) and n is a dimensionless exponent

$$r = k\{C\}^n. \tag{10}$$

One possibility is to fit k and n such that permeability trends fit experiments for a specific acid injection rate and concentration. If the same k and n are also valid for other experiments using different injection rates or concentrations, the model probably captures the underlying phenomena effectively.

The above approach still assigns reaction rate to pores based solely on their surface area and does not take into account their size or geometry. Since intra-pore diffusion is neglected (by assuming it happens infinitely quickly), the reaction rate in large pores will be overestimated compared to that in smaller pores. Therefore, it is possible that a coefficient to normalize the reaction rate against pore size could improve fits (equation 11).

$$r = \frac{V_{char}}{V_{Pore}} k\{C\}^n. \quad (11)$$

V_{pore} is the volume of an individual pore. V_{char} is some "characteristic" pore volume for which the reaction rate is appropriate. For example, this could be the median pore volume. However, in practice, both V_{char} and k would be effectively lumped into the same fitted coefficient. The important detail is that reaction rate is reduced as pore volume increases. A similar scheme could also punish the pore's reaction for very low convection rates. However, the overall goal would be to fit the data with as few complicating coefficients as possible.

Improve Pore Dissolution Model

The current merging approach is tolerably cheap from a computational perspective. A more physically accurate alternative is network re-extraction, but this is almost certainly unfeasible. Therefore, there is not likely to be a completely rigorous way to simulate matrix dissolution in a timely manner.

The current pore merging model is based on a set of simple common-sense heuristics. There are many other physically plausible rulesets that could govern the pore merging process that might yield better results. For example, currently pores are allowed to grow ad infinitum, absorbing any number of neighboring pores. This creates very large pores under face dissolution, and allows for pore geometry to grow outside the domain. One possible solution is to allow pores to only grow to a certain maximal volume and assign very large conductivity to throats connecting sufficiently large pores.

In addition to the pore merging algorithm, the way in which dissolved volume is translated into surface area and allocated to increase throat conductivity can also be examined. Currently, surface area is allocated to throats based on their existing conductivity. Allocating weighted proportionately to the incoming flow rate or incoming mols of acid is another possibility. Overall this modeling decision influences the significance of pore-scale heterogeneity, since it determines the extent to which large throats become larger.

Since the methodology and thresholds for merging pores are arbitrary, it is proposed that COMSOL simulations be used to identify the best rules. Flow between two spherical pores connected by a single throat can be solved repeatedly for various levels of dissolution. When they overlap, their space will automatically merge and flow will continue between them. Using this data one can determine what the best threshold for pore merging is, and what the best rules for intermediate cases are (such as when two pores barely begin to overlap).

Optimal Breakthrough Strategies

Existing simulations on single networks consistently show an optimal injection rate for a given acid type. However, optimal injection rates obtained thus far are not independent of scale. Some experimental research (Cohen et al. 2008) suggests injection rate should be independent of domain size above a certain scale (about 1"x6") as boundary effects diminish. Using mortar coupling to go to very large scales will be instrumental in testing this hypothesis. It will be very important to determine whether injection strategy is independent of domain size.

Fredd and Fogler (1999) identified that several fluid/rock systems shared a similar optimal Damkohler number (.29). However, their definition of the Damkohler number is dependent upon many parameters difficult to quantify consistently, such as the final wormhole dimensions. Thankfully, the Damkohler number, defined as the ratio of dissolution to convection, can be computed directly during network simulations. For any timestep, the amount of acid entering the domain is known, and the amount of acid reacted is also known. In principle this means that the Damkohler number could change as a function of time. However the Damkohler number stabilized quickly in a handful of simulations exploring this concept. Therefore, the possibility of collapsing many different fluid/rock systems onto a single characteristic dissolution curve will be investigated and compared with Fredd and Fogler's (1998b) finding of $Da_{opt} = 0.29$.

Thus far, we have only considered the optimal injection strategy as a fixed rate and concentration of acid. In field practice, however, it is common to inject at a fixed pressure rather than injection rate. In the absence of diverters, this means that injection rate must increase over time. For example, the "Maximized Pressure Differential and Injection Rates" (MAPDIR) technique (Paccaloni, 1995) was shown effective in a large number of field trials. Prima facie, it seems likely that the injection rate to best initiate the wormhole at the wellbore would be different from the best injection rate to extend wormholes several feet out into the reservoir. Therefore, it is unlikely that injecting at a single rate is actually the optimal overall strategy. A variety of injection strategies, including MAPDIR, could be investigated and compared under both linear and radial flow regimes.

Non-Newtonian Fluids

Self-diverting acids are popular choices for many fields. It is worth investigating under what conditions self-diverting acids are superior to choices to conventional fluids. Afsharpoor's (Pending) model for viscoelastic fluids should be straightforward to implement, as it only involves modifications to the pressure equation. The relationship between pressure drop and flow rate is shown in equation 12. The parameters in equation 12 are complicated but analytical functions of pore geometry parameters such as the hydraulic conductivity and aspect ratio. Simulations on viscoelastics can likely be validated via experiments.

$$\Delta P_{total} = \frac{\mu_{eff}}{G} Q[1 + bDe^3 + aln(1 + De)]. \quad (12)$$

References

Al-Raoush, Riyadh, Karsten Thompson, and Clinton S. Willson. "Comparison of network generation techniques for unconsolidated porous media." *Soil Science Society of America Journal* 67.6 (2003): 1687-1700.

Al-Dahlan, M. N., and H. A. Nasr-El-Din. "A new technique to evaluate matrix acid treatments in carbonate reservoirs." *SPE International Symposium on Formation Damage Control*. 2000.

Bartko, Kirk, et al. "Effective Matrix Acidizing in Carbonate Reservoir-Does Perforating Matter?." *SPE Middle East Oil and Gas Show and Conference*. 2007.

Bazin, B., C. Roque, and M. Bouteca. "A Laboratory Evaluation of Acid Propagation in Relation to Acid Fracturing: Results and Interpretation." *SPE European Formation Damage Conference*. 1995.

Bekri, S., J. F. Thovert, and P. M. Adler. "Dissolution of porous media." *Chemical engineering science* 50.17 (1995): 2765-2791.

Bryant, Steven L., David W. Mellor, and Christopher A. Cade. "Physically representative network models of transport in porous media." *AIChE Journal* 39.3 (1993): 387-396.

Cohen, Charles Edouard, et al. "From pore scale to wellbore scale: impact of geometry on wormhole growth in carbonate acidization." *Chemical Engineering Science* 63.12 (2008): 3088-3099.

Fatt, Irving. "The network model of porous media I. Capillary pressure characteristics." *Trans. AIME* 207.7 (1956): 144-159.

Fredd, C. N., and H. Scott Fogler. "Alternative stimulation fluids and their impact on carbonate acidizing." *SPE Journal* 3.1 (1998a): 34-41.

Fredd, Christopher N., and H. Scott Fogler. "Influence of transport and reaction on wormhole formation in porous media." *AIChE journal* 44.9 (1998b): 1933-1949.

Fredd, C. N., and H. S. Fogler. "Optimum conditions for wormhole formation in carbonate porous media: Influence of transport and reaction." *SPE Journal* 4.3 (1999): 196-205.

Glover, Martin C., and James A. Guin. "Dissolution of a homogeneous porous medium by surface reaction." *AIChE Journal* 19.6 (1973): 1190-1195.

Golfier, F., et al. "Acidizing carbonate reservoirs: numerical modelling of wormhole propagation and comparison to experiments." *SPE European Formation Damage Conference*. 2001.

Golfier, F., et al. "On the ability of a Darcy-scale model to capture wormhole formation during the dissolution of a porous medium." *Journal of fluid Mechanics* 457.213 (2002): C254.

Gong, M., and A. El-Rabaa. "Quantitative model of wormholing process in carbonate acidizing." *SPE Mid-Continent Operations Symposium*. 1999.

Hoefner, M. L., and H. S. Fogler. "Fluid-velocity and reaction-rate effects during carbonate acidizing: application of network model." *SPE production engineering* 4.1 (1989): 56-62.

Huang, TianPing, A. D. Hill, and R. S. Schechter. "Reaction rate and fluid loss: The keys to wormhole initiation and propagation in carbonate acidizing." *International Symposium on Oilfield Chemistry*. 1997.

Huang, T., L. Ostensen, and A. Hill. "Carbonate matrix acidizing with acetic acid." *SPE International Symposium on Formation Damage Control*. 2000.

Hung, K. M., A. D. Hill, and K. Sepehrnoori. "A mechanistic model of wormhole growth in carbonate matrix acidizing and acid fracturing." *Journal of petroleum technology* 41.1 (1989): 59-66.

Kang, Qinjun, et al. "Lattice Boltzmann simulation of chemical dissolution in porous media." *Physical Review E* 65.3 (2002): 036318.

Li, Li, Catherine A. Peters, and Michael A. Celia. "Upscaling geochemical reaction rates using pore-scale network modeling." *Advances in Water Resources* 29.9 (2006): 1351-1370.

Lichtner, P. C., and D. M. Tartakovsky. "Stochastic analysis of effective rate constant for heterogeneous reactions." *Stochastic Environmental Research and Risk Assessment* 17.6 (2003): 419-429.

Lund, Kasper, et al. "Acidization II. The dissolution of calcite in hydrochloric acid." *Chemical Engineering Science* 30.8 (1975): 825-835.

Lungwitz, Bernhard, et al. "Diversion and cleanup studies of viscoelastic surfactant-based self-diverting acid." *SPE Production & Operations* 22.1 (2007): 121-127.

Maheshwari, Priyank, and Vemuri Balakotaiah. "3D Simulation of Carbonate Acidization with HCl: Comparison with Experiments." *2013 SPE Production and Operations Symposium*. 2013.

Majdi, AL-Mutawa, et al. "Field cases of a zero damaging stimulation and diversion fluid from the carbonate formations in north kuwait." *International Symposium on Oilfield Chemistry*. 2003.

Mehmani, Yashar, et al. "Multiblock Pore-Scale Modeling and Upscaling of Reactive Transport: Application to Carbon Sequestration." *Transport in Porous Media* 95.2 (2012): 305-326.

Mohamed, S., H. Nasr-El-Din, and Y. Al-Furaidan. "Acid stimulation of power water injectors and saltwater disposal wells in a carbonate reservoir in Saudi Arabia: Laboratory testing and field results." *SPE Annual Technical Conference and Exhibition*. 1999.

Nasr-El-Din, Hisham, et al. "Lessons Learned and Guidelines for Matrix Acidizing with Viscoelastic Surfactant Diversion in Carbonate Formations." *SPE Annual Technical Conference and Exhibition*. 2006.

Navarrete, R. C., et al. "Emulsified acid enhances well production in high-temperature carbonate formations." *European Petroleum Conference*. 1998.

Paccaloni, Giovanni. "A new, effective matrix stimulation diversion technique." *Old Production & Facilities* 10.3 (1995): 151-156.

Panga, Mohan KR, Murtaza Ziauddin, and Vemuri Balakotaiah. "Two-scale continuum model for simulation of wormholes in carbonate acidization." *AIChE journal* 51.12 (2005): 3231-3248.

Patzek, T. W., and D. B. Silin. "Shape factor and hydraulic conductance in noncircular capillaries: I. one-phase creeping flow." *Journal of colloid and interface science* 236.2 (2001): 295-304.

Quinn, Michael Anthony, Larry W. Lake, and Robert S. Schechter. "Designing effective sandstone acidizing treatments through geochemical modeling." *Old Production & Facilities* 15.1 (2000): 33-41.

Schechter, R. S., and J. L. Gidley. "The change in pore size distribution from surface reactions in porous media." *AIChE Journal* 15.3 (1969): 339-350.

Smith, C. F., and A. R. Hendrickson. "Hydrofluoric acid stimulation of sandstone reservoirs." *Journal of Petroleum Technology* 17.2 (1965): 215-222.

Sun, Tie, Yashar Mehmani, and Matthew T. Balhoff. "Hybrid multiscale modeling through direct substitution of pore-scale models into near-well reservoir simulators." *Energy & Fuels* 26.9 (2012): 5828-5836.

Szymczak, P., and A. J. C. Ladd. "Wormhole formation in dissolving fractures." *Journal of Geophysical Research: Solid Earth (1978–2012)* 114.B6 (2009).

Talbot, Malcolm, and Rick Gdanski. "Beyond the Damkohler Number: A New Interpretation of Carbonate Wormholing." *Europec/EAGE Conference and Exhibition*. 2008.

Thomas, R. L., Alan Saxon, and A. W. Milne. "The Use of Coiled Tubing During Matrix Acidizing of Carbonate Reservoirs Completed in Horizontal, Deviated, and Vertical Wells." *Old Production & Facilities* 13.3 (1998): 147-162.

Wang, Y., A. D. Hill, and R. S. Schechter. "The optimum injection rate for matrix acidizing of carbonate formations." *SPE Annual Technical Conference and Exhibition*. 1993.

Walsh, Mark, Larry Lake, and Robert Schechter. "A description of chemical precipitation mechanisms and their role in formation damage during stimulation by hydrofluoric acid." *Journal of Petroleum Technology* 34.9 (1982): 2097-2112.

Walsh, M. P., et al. "Precipitation and dissolution of solids attending flow through porous media." *AIChE Journal* 30.2 (1984): 317-328.